Fabrication and characterization of NiO nanoparticles deposited via reactive DC magnetron sputtering technique

H. A. Abbas[a], A. J. Rahma[b,*], H. F. Oleiwi[c]
[a]*Department of postgraduate Affairs, University of Baghdad, Baghdad, Iraq*
[b]*Middle Technical University, Engineering Technical Collage- Baghdad, Fuel and Energy Department, Iraq*
[c]*Department of Physics, College of Science for Women, University of Baghdad, Iraq.*

Nickel oxide (NiO) nanostructure was successfully prepared via reactive DC magnetron sputtering on the soda-lima glass substrate, which can be used for various applications. X-ray diffraction (XRD) investigations were used to evaluate NiO with two annealing durations. The results revealed that the deposited films had a cubic structure and polycrystalline nanoparticles. A significant polycrystalline structure could be seen in the sputtered films as a diffraction peak oriented toward NiO (200). Field-emission Scanning Electron Microscopy (FE-SEM) analysis identified the surface morphology of NiO nanoparticles prepared at two different annealing times with the two average sizes (24 and 32 nm) respectively. The samples' roughness was assessed using atomic force microscopy (AFM). Increased annealing time was shown to result in a decrease in grain size. The energy band gap (Eg) expanded with increasing annealing time, according to UV-visible spectroscopy (UV-Vis). FTIR spectroscopy was used to determine the functional groups of NiO nanoparticles and their bonding nature. The results indicate that optical characterizations are more sensitive to the annealing period.

(Received May 22, 2024; Accepted September 16, 2024)

Keywords: NiO nanoparticle, DC magnetron sputtering, AFM, SEM

1. Introduction

With an electronic structure that can exhibit metallic, semiconductor, or insulator features, metal oxides are capable of adopting a wide range of structural geometries, giving them a variety of chemical and physical properties [1]. The most crucial functional materials for chemical and biological sensing and transmission are metal oxides [2, 3]. Nickel (II) oxide is the chemical compound having the formula NiO. Although (III) oxide, Ni_2O_3, and NiO_2 have been suggested, it is significant for being the only nickel oxide that has been thoroughly described. The inorganic form of NiO is exceptionally rare. It belongs to the category of basic metal oxides [4]. Annually, several million kilograms of variable quality are manufactured, primarily as an intermediary in the creation of nickel alloys [5]. Semiconducting metal oxide NiO is frequently used as a representation of p-type material [6]. NiO has a rhombohedra or cubic crystal structure at ambient temperature [7, 8], although the most noticeable structure was cubic structure. With an absorption edge in the near UV-visible range, NiO exhibits a large Eg of 3.6 to 4.0 eV [9, 10]. It is an insulator at room temperature, exhibits functional properties, and is a potential candidate for a number of applications, such as UV optoelectronic devices [11], positive electrodes in batteries [12], solar thermal absorbers [13], fuel cells, catalysts, gas sensing devices [14], and electrochromic display devices, among others [15]. The p-type semiconductor property of NiO nanostructures is found when nickel vacancies and interstitial oxygen atoms are produced in NiO crystallites during film growth [9, 16]. Superior toughness and electrochemical stability, cheap material prices, cyclic stability potential as an ion storage material, high spin optical density, and

* Corresponding author: aseel.jabbar@mtu.edu.iq
https://doi.org/10.15251/DJNB.2024.193.1309

versatility in manufacturing methods are just a few of its many appealing attributes. NiO films can be produced by a variety of chemical and physical techniques, including spray pyrolysis [17], electron beam evaporation [18] , pulsed laser deposition , plasma assisted chemical vapor deposition [19], reactive sputtering [4], and magnetron sputter deposition are instances of both chemical and physical methods that can be used to produce NiO films [6, 20, 21] .

In this study, since it offers various advantages over evaporation methods for film deposition, such as not directly heating the material, magnetron sputter deposition was utilized to create NiO nanostructures. Because of this, there is no interaction between the source and the crucible [22, 23]. Usually, increased attraction is caused by the fact that sputtered atoms have a larger average arrival energy at the substrate (approximately 10 eV). The impacting ion flux has a linear relationship with the deposition rate, but the source temperature has an exponential relationship with the deposition rate in evaporation.[24]. The most popular method has been reactive sputtering. The properties of the films are influenced by sputtering factors such as reactive sputtering gas ratio, sputtering pressure, RF power, and substrate temperature. The annealing duration has a greater influence on characterizations of NiO nanoparticles [8].

2. Experimental method

Using a DC reactive magnetron sputtering technique, NiO nanostructures were deposited from a pure nickel (99.99%) target (100 mm in diameter and 3 mm in thickness) in a mixture of oxygen and argon (50/50) gases on glass substrates. In the current study, NiO thin nanostructures were formed at different annealing temperatures (pristine, 2 hours, and 4 hours) at 450 ^{o}C, while maintaining a consistent target to substrate distance. In Table 1, the deposition parameters that are used to create NiO nanostructures are listed. At a sputtering gas pressure of 610^{-2} mbar, argon gas was injected after the sputtering chamber had been evacuated to less than 510^{-5} mbar, with the discharge current being 15–30 mA and the voltage being 0.6–1 KV. The films were deposited on a glass substrate with (2×2) cm^2 dimensions with an optical transmission of approximately 95. The system was pumped down to its base pressure, which was reached before each deposit and is around 810^{-2} mbar. By delivering a negative voltage to the cathode, argon is delivered into the chamber as a precursor to ignite the plasma. The target is pre-sputtered in Ar for at least 15 minutes before to the deposition of each layer in order to eliminate any surface oxide from in front of the target.In order to calculate the proper stoichiometry and thickness for the sample, oxygen flow rate is essential. Sputtering is carried out using a steady voltage. The target is preconditioned with the reactive gases at the selected deposition condition before being exposed to a substrate. A needle valve is used to enter the Ar/O_2 mixture into the chamber at the specified pressure based on the cathode voltage as shown by the DC power supply and the Ar/O_2 ratio as calculated by the flow meter. For the experiment period, the deposition time is 90 minutes. These variables distinguish between different sputtering depositions.

Table 1. NiO films' deposition parameters.

No.	Deposition conditions	Range
1	Target-substrate distance	3 cm
2	Ultimate pressure	5×10^{-6} mbar
3	Sputtering pressure	8×10^{-2} mbar
4	Substrate temperature	473 k
5	Sputtering voltage	0.6 -1 k volt
6	Deposition time	90 min

3. Characterization techniques

Atomic force microscopy (AFM) type (AA3000) was used to analyze the sample surface topography and evaluate the distribution rate of the crystal size of NiO nanostructure. The surface morphology of NiO nanoparticles was investigated using SEM (ZEISS Supra 55 VP, Germany). By using a Cu K radiation (1.54 Aº) equipped X-ray diffractometer from SHIMADZU Japan, structural characteristics of the sputtered films were examined. A UV-Vis spectrometer (Perkin Elmer Lambda 1800) was used to measure the optical characteristics over the wavelength range of 300 to 1100 nm. FTIR spectra were taken on a JASCO 640 plus infrared spectrometer in the range of 4000–4000 cm^{-1}.

4. Results and discussions

The AFM images of the NiO nanocrystalline at various annealing durations (pristine, 2 hours and 4 hours) are shown in Fig.1. The images clearly show the films' uniform surface and good density. Also, as shown in Table 2, when the film was annealed for two hours, the particle size of the samples produced by the process reduced from 79.95 nm to 76.88 nm, resulting in a decrease in surface roughness. In a while, after 4 hours of annealing, the samples' roughness increased [25]. The sample's diameter distribution (annealed for 2 hours) is shown in Fig. 2. The average particle size of the samples dropped when annealing duration incresed, which may be related to an increase in film crystallanity. Moreover, as the annealing time increased, the root mean square (RMS) roughness reduced. In Table 2, the average grain size and surface roughness were listed.

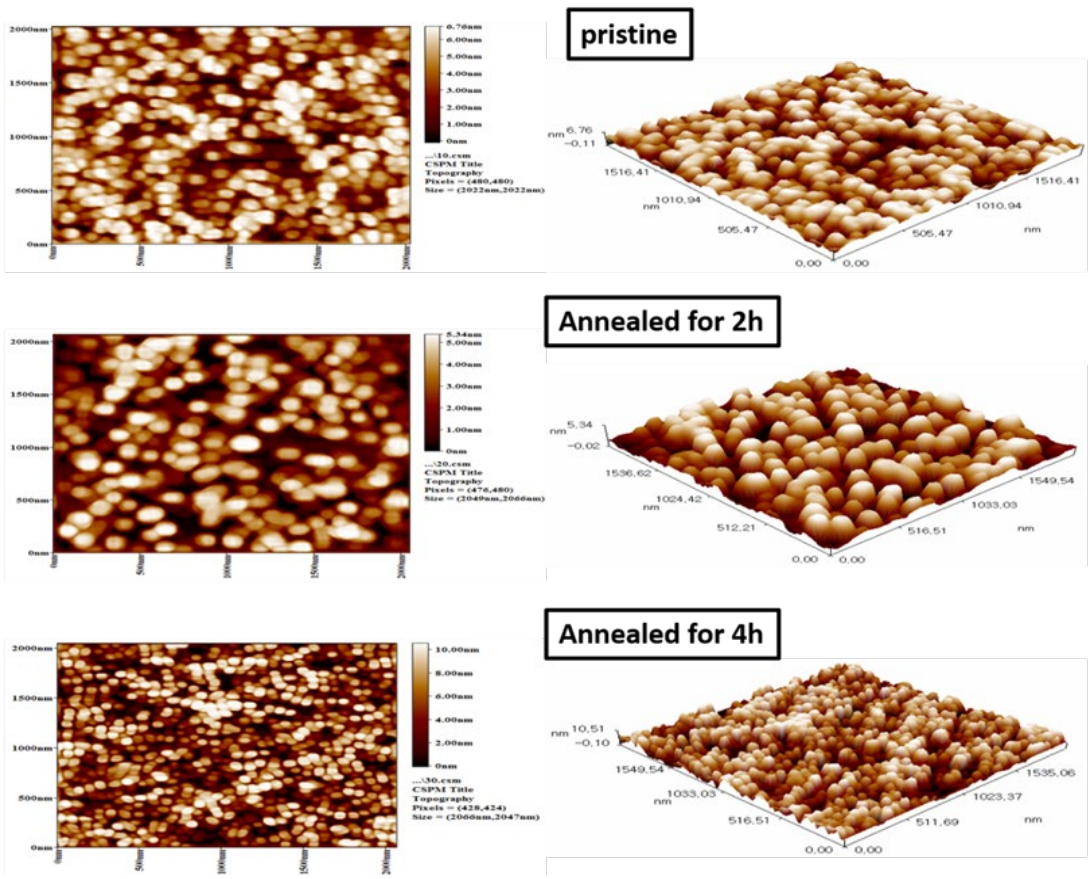

Fig. 1. AFM images of NiO nanostructures with different annealing time.

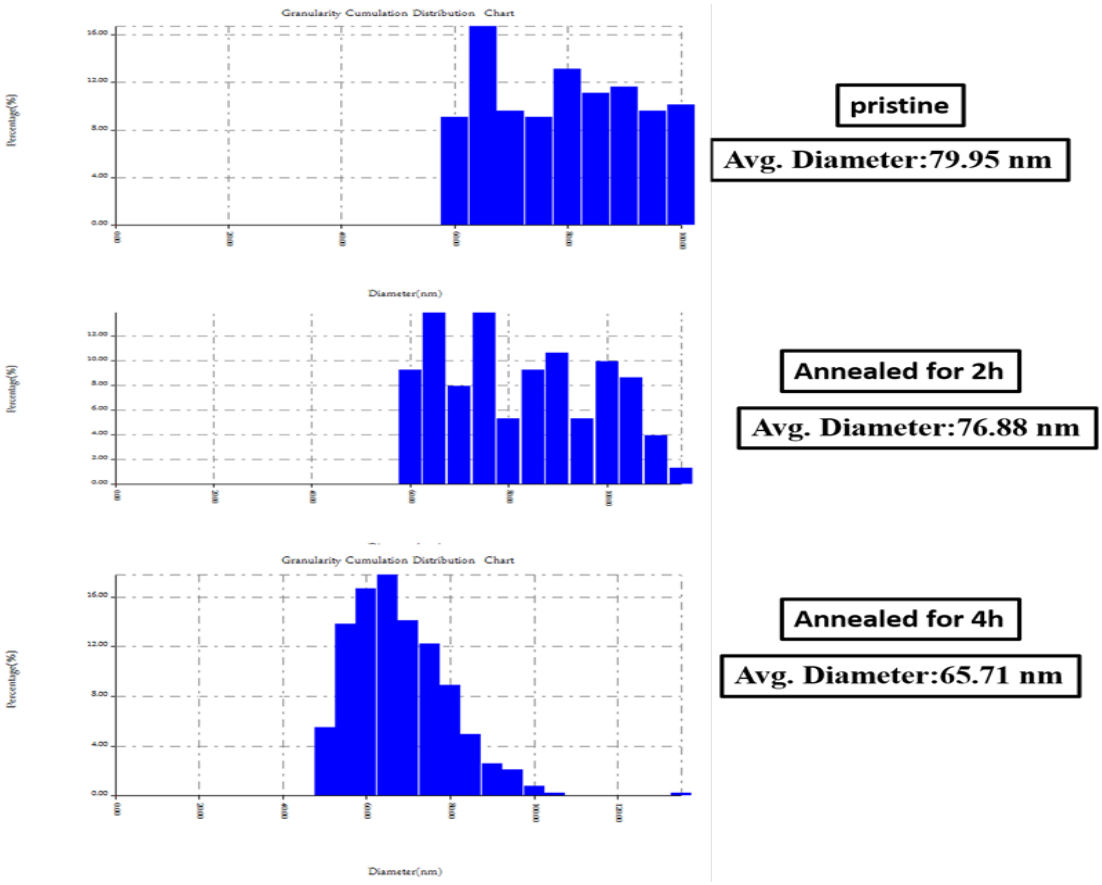

Fig. 2. Distribution chat of NiO nanostructures with different annealing time.

Table 2. AFM characteristics of NiO nanostructures at various annealing temperatures

Annealing	Roughness (nm)	Average grain size (nm)
Pristine	1.51	79.95
Annealed for 2h	1.33	76.88
Annealed for 4h	2.65	65.71

Fig. 3. and Fig (4) show SEM images of NiO nanoparticles with magnification of 5000 after two different annealing time (2 and 4 hr.) and it was indicated a spherical shapes of particles in the average size 24 and 32 nm respectively [26].

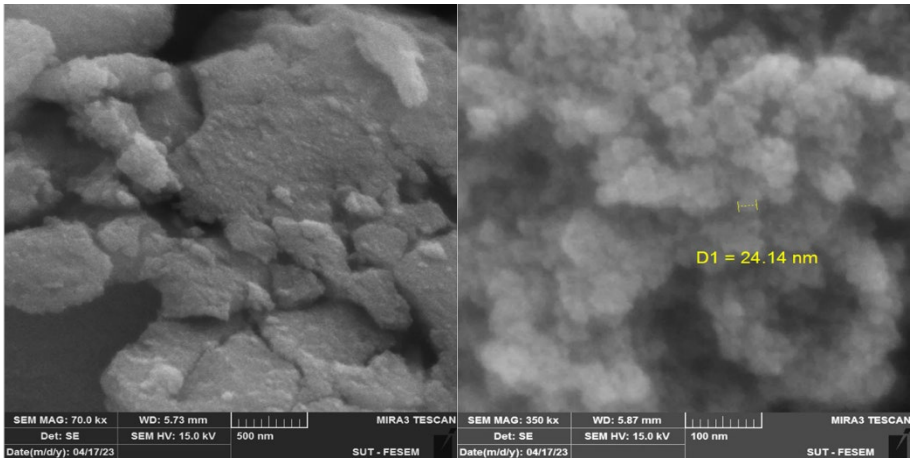

Fig. 3. SEM images of NiO nanoparticles at 2hr. annealing time.

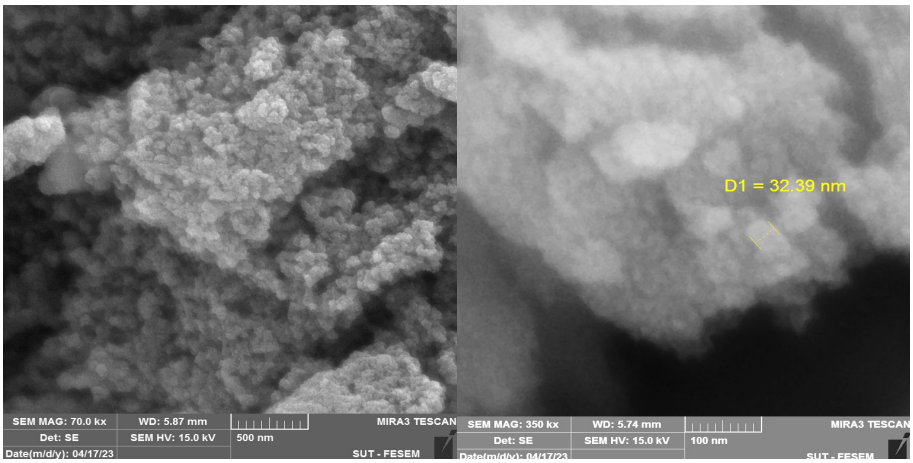

Fig. 4. SEM images of NiO nanoparticles at 4hr. annealing time.

The XRD patterns of NiO nanostructures for various annealing times are shown in Fig. 5. There are only the two classic diffraction peaks (111 and 200) that can be seen; no other peaks are present. The dominating peak (111), which is more intense than the other peaks and thus the most noticeable peak for all structures, and the peaks of reflections demonstrate the polycrystalline nature of the nanostructures. The peak intensities reduced after 4 hours of annealing, this could be due to the rise of crystal orientations. The peak intensity and sharpness rose when the film was annealed for two hours, and this improvement was achieved about by the crystallite size (D) dropping from 79.95 nm to 76.88 nm, which determined using Scherrer's equations [3, 27]:

$$D= 0.9\ \lambda/\ \beta\ \cos\theta \qquad (1)$$

where β is the full width at half maximum (FWHM) of a certain diffraction peak and λ is the X-ray incident wavelength.

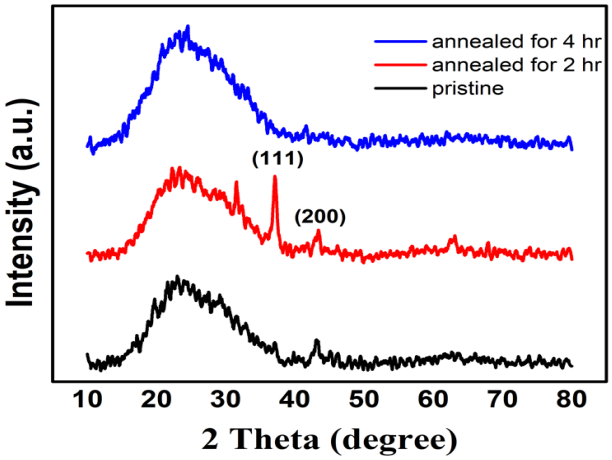

Fig. 5. XRD pattern of NiO nanostructures with different annealing time.

Fig. 6 shows the optical absorption spectra of the NiO nanostructures with different annealing time (without annealing, annealing for 2 hr and annealing for 4 hr). There appeared a broad absorption band in the spectral range of 300–400 nm. The main role of absorption in the region (324-344 nm) occurs near absorption edge of NiO nanostructures. Fig. 6 shows that the annealing time (2hr) influence at absorption spectrum of NiO nanostructures [28]. This could be attributed to high absorption from oxide layer or by the nickel and oxygen impurities which are diffused in band gap of NiO films.

The curves for varying annealing time have the straight portion of the $(\alpha h\upsilon)^2$ vs. $h\upsilon$ at $h\upsilon$ and the intercept with the x-axis at $\alpha h\upsilon=0$, as illustrated in Fig. 8, have been used to compute the Eg of NiO nanostructure with varying annealing time. With 2 hour increase in annealing time, Eg values dropped from 3.69 to 3.6 eV [29]. Impurities and structural defects like oxygen vacancies and interstitials can affect the energy band gap values. Hence, the diffusion of aluminum and oxygen, which inhabit interstitial spaces between NiO lattices, could result in diminishing Eg values, as seen in Fig. 9. Eg rise to 4 eV when the sample was annealed for 4 hours. The variation of Eg with various annealing time is illustrated in Fig. 9. As the annealing time was increased, it was seen that the Eg initially reduced and then increased.

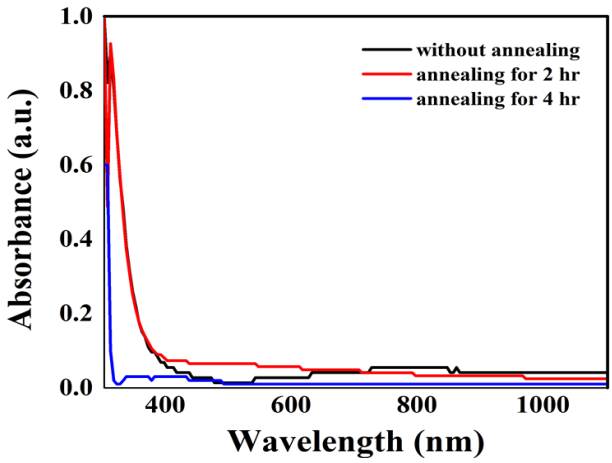

Fig. 6. Absorption spectra of the NiO films with different annealing time.

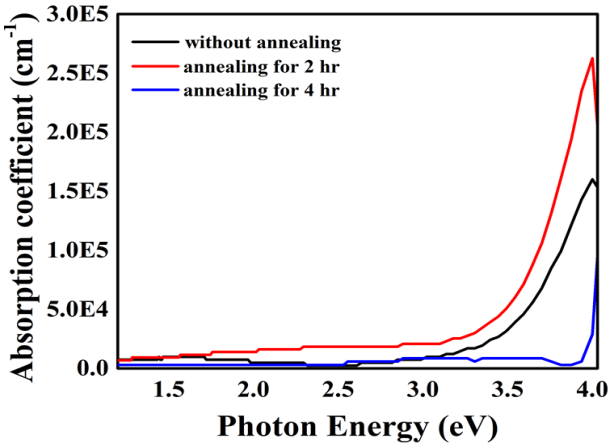

Fig. 7. Absorption coefficient of the NiO films with different annealing time.

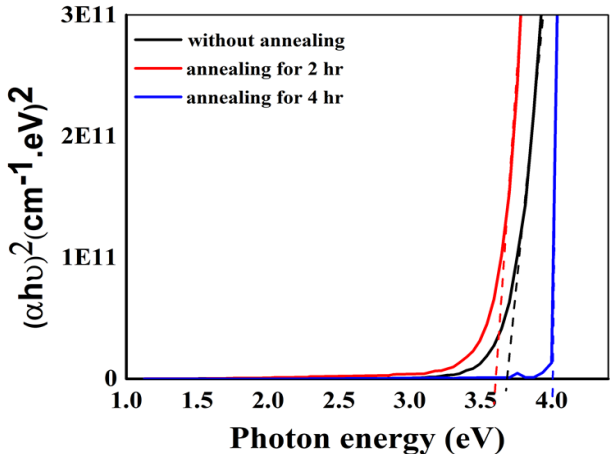

Fig. 8. Energy band gap of the NiO nanostructure with various annealing time.

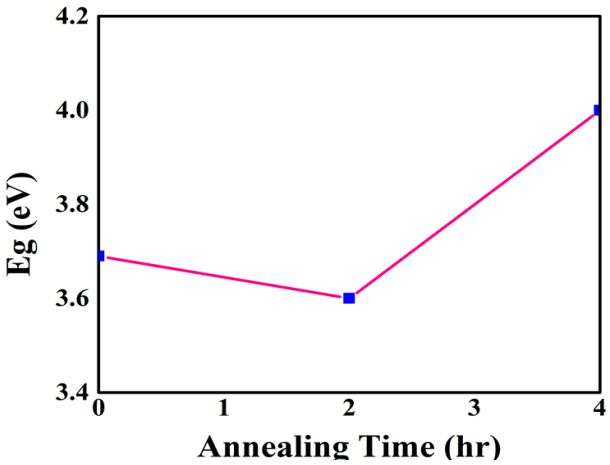

Fig. 9. The variation of Eg for NiO thin films.

Fourier Transform Infrared Spectroscopy (FTIR) was used to investigate the bond analysis of NiO nanoparticles at two different annealing time (2 and 4hr.). The samples powder were mixing with KBR and pressed in a pellet and putted in the device to show the bonds in the range of 500 to 4000cm^{-1}. Fig. 10 and 11 explain the stretching and vibration bonds. In Fig. 10, the (O-H) groups appeared in 3471cm^{-1} and 1639cm^{-1} that attributed to hydroxyl group. The stretching bond of (Ni-OH) appeared at (719cm^{-1}) and the vibration bond of (Ni-O) located at 483cm^{-1}. In Fig. 11 the (O-H) groups appeared in 3480cm^{-1} and 1645cm^{-1}. (Ni-OH) stretching bond were appeared at 729cm^{-1}and (Ni-O) at 495cm^{-1}. All these information indicated a pure of NiO nanoparticles [25].

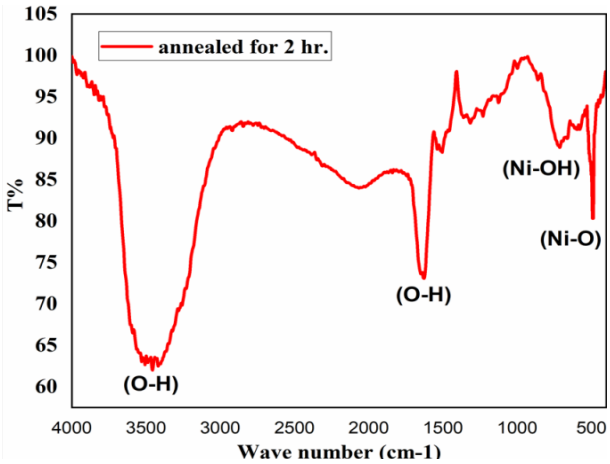

Fig. 10. FTIR spectra of NiO nanoparticles that prepared at 2hr. annealing time.

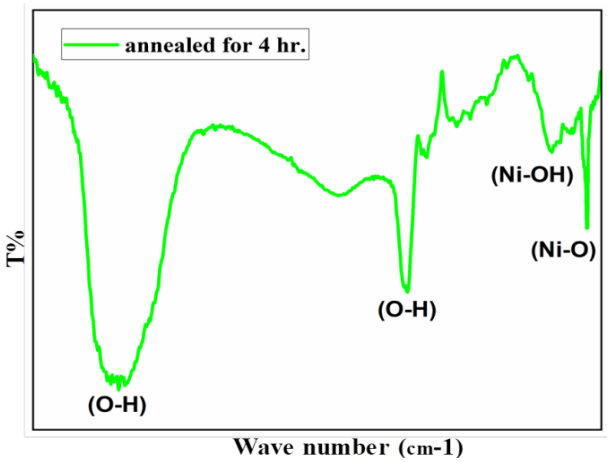

Fig. 11. FTIR spectra of NiO nanoparticles that prepared at 4hr. annealing time.

5. Conclusions

Dc reactive magnetron sputtering at varied annealing times was successful in depositing nanostructured Nickel oxide (NiO) nanostructures. Investigations were done into how the annealing period affected the morphological, structural, and optical properties. The crystalline nature and size of the particles dropped and subsequently rose with increasing annealing time, according to the XRD, SEM and AFM data. Yet, the AFM image analysis showed that the roughness levels fluctuate widely (within the range of 1.51–2.65 nm).SEM images indicate a spherical nanoparticles and nanoclusters in the average size (24 and 32nm) at (2 and 4hr.) of annealing time. NiO films displayed cubic structure and polycrystalline nature along the (111)

orientation. As the annealing time was extended, the optical transmittance and Eg of the samples first declined, then increased. When the nanostructure's annealing duration and grain size rose, Eg calculated using UV-Vis spectroscopy first reduced, then increased. FTIR spectrum confirm to pure NiO nanoparticles.

Acknowledgements

We especially thank the personnel of the University of Baghdad's Chemistry and Physics Laboratory.

References

[1] A.Singh, S. Dubey, and H. K. J. N. Dubey, Nanotechnology: The future engineering, 6(2), 230 (2019).
[2] M.Fernandez-Garcia, A. Martinez-Arias, J. C. Hanson, J. A. Rodriguez, Chemical reviews, 104, no. 9, pp. 4063-4104, (2004); https://doi.org/10.1021/cr030032f
[3] A. J. Rahma, H. F. Oleiwi, S. G. Khaleel, M. M. Mutter, IOP Publishing 1095, 1 (2007);
[4] Y.Zhao et al., Electrochimica Acta 367, 137457 (2021);
https://doi.org/10.1016/j.electacta.2020.137457
[5] M. A. M. Hussein, Sudan University of Science and Technology, (2016).
[6] Y.-J. Lin, T.-H. Su, P.-C. Kuo, and H.-C. Chang, Materials Chemistry and Physics 276, 125345 (2022); https://doi.org/10.1016/j.matchemphys.2021.125345
[7] F.I. Ezema, A. B. C. Ekwealor, R. U. Osuji, Superficies y vacío 21(1), 6 (2008).
[8] K.K. Purushothaman, G. Muralidharan, Solar Energy Materials and Solar Cells 93(8), 1195 (2009); https://doi.org/10.1016/j.solmat.2008.12.029
[9] H.J. M. Swagten, G. J. Strijkers, P. J. H. Bloemen, M. M. H. Willekens, W. J. M. De Jonge, Physical Review B 53(14), 9108 (1996); https://doi.org/10.1016/j.solmat.2008.12.029
[10] L.Qi, B. Cheng, W. Ho, G. Liu, J. J. C. Yu, ChemNanoMat 1(1), 58 (2015;) https://doi.org/10.1002/cnma.201400013
[11] J. Shi, J. Zhang, L. Yang, M. Qu, D. C. Qi, K. H. J. A. M. Zhang, Advanced Materials 33(50), 2006230 (2021); https://doi.org/10.1002/adma.202006230
[12] N.R. Glavin et al., Advanced Materials 32(7), 1904302 (2020);
https://doi.org/10.1002/adma.201904302
[13] Y.Tian, X. Liu, A. Ghanekar, Y. J. A. E. Zheng, Applied Energy 281, 116055 (2021);
https://doi.org/10.1016/j.apenergy.2020.116055
[14] G.Eranna, B. Joshi, D. Runthala, R. J. C. R. i. S. S. Gupta, Critical Reviews in Solid State and Materials Sciences 29(3-4), 111 (2004); https://doi.org/10.1080/10408430490888977
[15] S.Ibrahim, H. A. Abo-Mosallam, E. A. Mahdy, G. M. Turky, Journal of Materials Science: Materials in Electronics 33(13), 10596 (2022).
[16] T.P. Mokoena, Z. P. Tshabalala, K. T. Hillie, H. C. Swart, D. E. J. A. S. S. Motaung, Applied Surface Science 525, 146002 (2020); https://doi.org/10.1016/j.apsusc.2020.146002
[17] M.Aftab, M. Z. Butt, D. Ali, F. Bashir, T. M. Khan, Optical Materials 119, 111369 (2021);
https://doi.org/10.1016/j.optmat.2021.111369
[18] T.Abzieher et al., Advanced Energy Materials 9(12), 1802995 (2019) ;
https://doi.org/10.1002/aenm.201802995
[19] C.Vallée et al., Journal of Vacuum Science and Technology A: Vacuum, Surfaces, and Films 38(3), 033007 (2020)
[20] A.A. A. Alwahab, N. J. Jubier, J. F. Odah, AIP Publishing LLC 2437, 020102
[21] A.Ben Gouider Trabelsi, F. H. Alkallas, A. Ziouche, A. Boukhachem, M. Ghamnia, H. Elhouichet, Crystals 12(5), 692 (2022) ; https://doi.org/10.3390/cryst12050692

[22] N. Abid et al., Advances in Colloid and Interface Science 300, 102597 (2022); https://doi.org/10.1016/j.cis.2021.102597
[23] I. R. Agool, M. K. Khalaf, S. H. Abd Muslim, R. N. J. E. Talaq, Engineering and Technology Journal 33(6) Part (B) Scientific, (2015); https://doi.org/10.30684/etj.2015.116476
[24] A. M. Reddy, A. S. Reddy, K.-S. Lee, P. S. Reddy, Ceramics International 37(7), 2837 (2011); https://doi.org/10.1016/j.ceramint.2011.04.121
[25] A. Rahdar, M. Aliahmad, Y. Azizi, NiO nanoparticles: synthesis and characterization, 2015.
[26] M. J. J. o. N. R. Bonomo, Journal of Nanoparticle Research 20(8), 222 (2018); https://doi.org/10.1007/s11051-018-4327-y
[27] Aseel J. Rahma, Hind F. Oleiwi, Haider A. Abbas, J Nanostruct 13(3), 673 (2023)
[28]Hind Fadhil Oleiwi, Aseel J. Rahma, Siham I Salih, Ammar A.Beddai, Baghdad Science Journal 21(5), 1702, (2024); https://doi.org/10.21123/bsj.2023.8089
[29] M. Ghougali, O. Belahssen, A. Chala, Structural, optical and electrical properties of NiO nanostructure thin film, (2016).